CONTROLS ON EARLY CRETACEOUS DESERT SEDIMENT PROVENANCE IN SW GONDWANA, BOTUCATU FORMATION, BRAZIL

Bertolini, G.[1,2], Marques, J.C.[2], Hartley, A.J.[1], Da-Rosa, A.A.S[3], Scherer, C.M.S[2], Basei, M.A.S.[4], Frantz, J.C.[2]

[1] Geology & Petroleum Geology, King's College, University of Aberdeen, Aberdeen, AB24 3FX, UK (E-mail: gabertol@gmail.com)

[2] Instituto de Geociências, Universidade Federal do Rio Grande do Sul, Porto Alegre 90040-060, Brazil

[3] Departamento de Geociências, Universidade Federal de Santa Maria, Av. Roraima, 1000 Predio 17,Santa Maria, RS 97105-900, Brazil

[4] Instituto de Geociências, Universidade de São Paulo, São Paulo 05508- 80, São Paulo, Brazil

Abstract

The Lower Cretaceous Botucatu Formation records the development of widespread dry-aeolian desert sedimentation throughout the Paraná Basin in SW Gondwana. To reconstruct the provenance of the aeolian sediment, petrography, granulometric analysis and U-Pb detrital zircon have been determined from along the southern basin margin in Rio Grande do Sul state (S Brazil) and Uruguay (Tacuarembó region). The dataset reveals a mean $Qt_{89}F_8L_3$, comprising very-fine to medium grained quartozose and feldspathatho-quartzose framework. Heavy mineral analysis reveals an overall dominance of zircon, tourmaline and rutile grains (mean ZTR_{84}) with sporadic garnet, epidote and pyrolusite occurrences. The detrital zircon U-Pb ages are dominated by Cambrian to Neoproterozoic (515-650 Ma), Tonian to Stenian (900-1250 Ma) and Orosirian to Rhyacian (1.8-2.2 Ga) material. The detrital zircon dataset demonstrates a significant lateral variation in sediment provenance: Cambrian to Neoproterozoic detrital zircons dominate in the east, while Tonian and Stenian and Orosirian to Rhyacian ages predominate in the west of the study area.

Sandstones are quartz-rich with dominantly durable ZTR heavy mineral suite, with subtle but statistically significant along strike differences in heavy mineral populations and detrital mineralogy which are thought to record local sediment input points into the aeolian system. The similar age spectra of Botucatu desert with proximal Paraná Basin units, the predominance of quartzose and ZTR components, suggests that recycling is the mechanism responsible for sediment supply to the Botucatu erg.

1. Introduction

Determining the origin and transport paths of sediment in aeolian systems is important for understanding how and why large accumulations of aeolian sediment are developed and preserved (Dickinson and Gehrels, 2003; Rahl *et al.*, 2003). Provenance studies of dune field sediment supply and erg sand-delivery systems reveal a range of desert sand supply mechanisms. For example sands in the Namib Desert are sourced by longshore drift from the Orange River delta (Garzanti *et al.*, 2014), sands in the Taklamakan Desert are supplied by fluvial systems draining the surrounding mountain ranges (Rittner *et al.*, 2016), and the Rub` Al Khali erg (Arabian Desert) is derived from a mix of sand sources including aeolian transport and deflation as well as fluvial, alluvial and coastal inputs (Farrant et al., 2019). In the rock record, a study of the Jurassic ergs of the Colorado Plateau was able to reconstruct a transcontinental SE-NW paleoriver and paleowind system responsible for transportation and dispersal of sediment in Laurentia (Dickinson and Gehrels, 2009). When studying the sedimentary record however, it is often difficult to properly reconstruct aeolian sediment supply systems due to the incompleteness of the succession and post-depositional diagenetic modification of the original mineralogy (McBride, 1985; Cardenas *et al.*, 2019). As a consequence, with the exception of the

Permian-Jurassic Colorado Plateau ergs (Dickinson and Gehrels, 2003; 2009 and 2010; Rahl *et al*. 2003), there is a lack of studies that address the reconstruction of sediment source terranes, sediment pathways, sediment mixing, recycling and transport distance in ancient large-scale ergs. To address this gap, we have undertaken a provenance analysis of the Botucatu Formation, a Cretaceous aeolian unit deposited across SW Gondwana.

The Cretaceous Botucatu dune field extended continuously across 1.5 million km^2 of the interior of the SW Gondwana Supercontinent and represents part of what was probably the most voluminous continuous dune field in Earth history (Scherer and Goldberg, 2007; Fig. 29). The Botucatu sand sea forms part of the intracratonic Paraná Basin-fill succession and represents the last phase of sedimentation in the Paraná Basin prior to break-up of the South American and African continents. The Paraná Basin developed across a wide range of different pre-Mesozoic basement terranes (Paleoproteorozoic to Cambrian) with differing ages and compositions. Consequently, when combined with previous work on paleowind directions, it should be possible to distinguish different provenance signatures in the Botucatu Formation. Previous studies of the formation (e.g. Bigarella and Salamuni, 1961) show that coarser sediment prevails in the southern part of the basin suggesting input from the south. In addition, the close proximity of the Botucatu to basement highs (e.g. the Rio-Grandense and Uruguayan Shields), may allow establishment of a direct source-to-sink connection. Sediment provenance studies from the southern part of the basin will therefore be important in reconstructing sediment routing systems, understanding controls on sediment supply and assessing the potential for first cycle input direct from basement terranes.

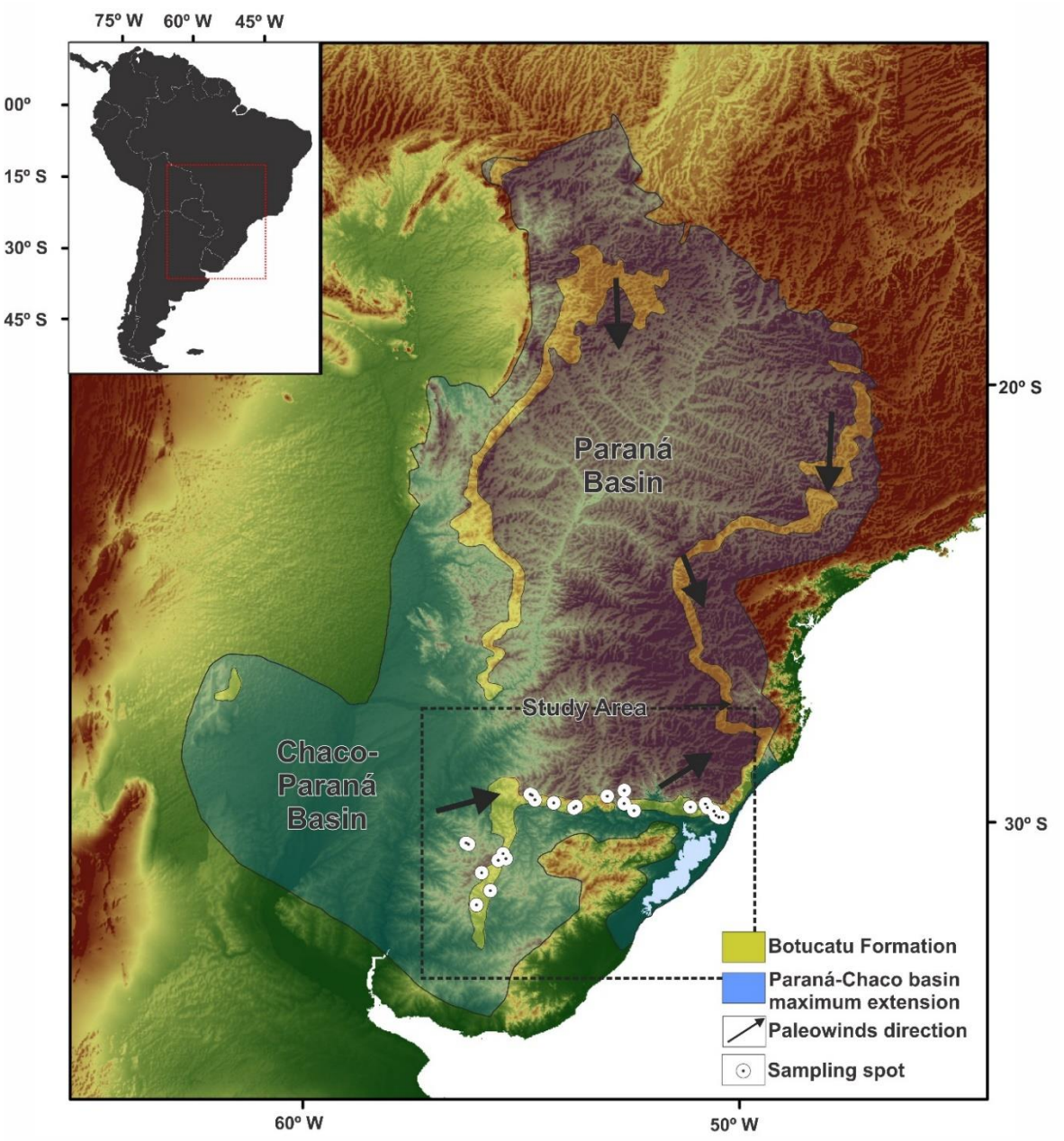

Figure 1- Botucatu desert extent in South America within the Paraná and Chaco-Paraná Basins with sample locations. The desert had a bimodal wind pattern, with southerly directions in low latitudes and NE-E directions in the study (Scherer, 2000; Scherer and Goldberg, 2007).

The primary objective of this study is to constrain and clarify the nature of the sediment source for the Botucatu dunes along a transect of the southern Paraná Basin margin (SE Brazil and Uruguay). Due to the continental scale of the aeolian system, the Botucatu Formation covers a number of distinct geologic terranes providing a wide range of potential sediment source areas and pathways. Provenance analysis utilizing

U-Pb detrital zircon geochronology, heavy mineral analysis, petrography, and granulometric analysis has been undertaken to ascertain if significant variations in sediment provenance signatures across the southern basin margin can be identified.

2. Geologic Context

The Botucatu Formation forms part of the intracratonic Paraná Basin fill succession - an 8 km thick (Zálan et al., 1990) sedimentary-magmatic package of Late Ordovician to Early Cretaceous age (Fig. 30). In the south (Brazil, Argentina, Paraguay), the basin-fill is divided into six supersequences (Milani *et al.*, 1998): Rio Ivaí (Ordovician-Silurian), Paraná (Devonian), Gondwana I (Carboniferous-Lower-Triassic), Gondwana II (Triassic), Gondwana III (Early Jurassic to Lower Cretaceous) and Bauru (Early Cretaceous). The Rio Ivaí, Paraná and Gondwana I supersequences represent marine and shoreline deposits. The Gondwana II, Gondwana III, and Bauru supersequences comprise terrestrial sediments and associated volcanic strata. The Botucatu Formation and the Serra Geral Formation form part of the Gondwana III supersequence, also known as the São Bento Group (Schneider *et al.*, 1973). The Botucatu paleoerg is overlain by 700-1700m of lava-flows from the Paraná-Etendeka Large Igneous Province (Serra Geral Formation). Interbedded basaltic lava flows and aeolian sediments indicate co-existence between, and a transition from, aeolian sedimentation to lava emplacement (Scherer, 2002).

The age of the top of the Botucatu Formation is constrained by overlying lavas of the Serra Geral Formation, which have yielded ages of 134.5 Ma ± 0.5 Ma (Valagininan) by Ar/Ar (Whole-rock grains/ plagioclase) and U-Pb methods (Zircon and Badeleeite) (Ernesto *et al.,* 1999; Thiede and Vasconcelos, 2010; Pinto *et al.,* 2011, Janasi *et al.,* 2011; Rossetti *et al.,* 2018, Baksi, 2018). The determination of the onset

of Botucatu deposition is imprecise due a lack of dated interbedded volcanics and/or palaeontological constraints. The Botucatu Formation overlies the Upper Jurassic Guará and Batovi Member (Soto and Perea, 2008; Perea *et al.,* 2009; Francischini *et al.,* 2015), suggesting an earliest Cretaceous age (Berriasian to Valanginian) for paleoerg accumulation.

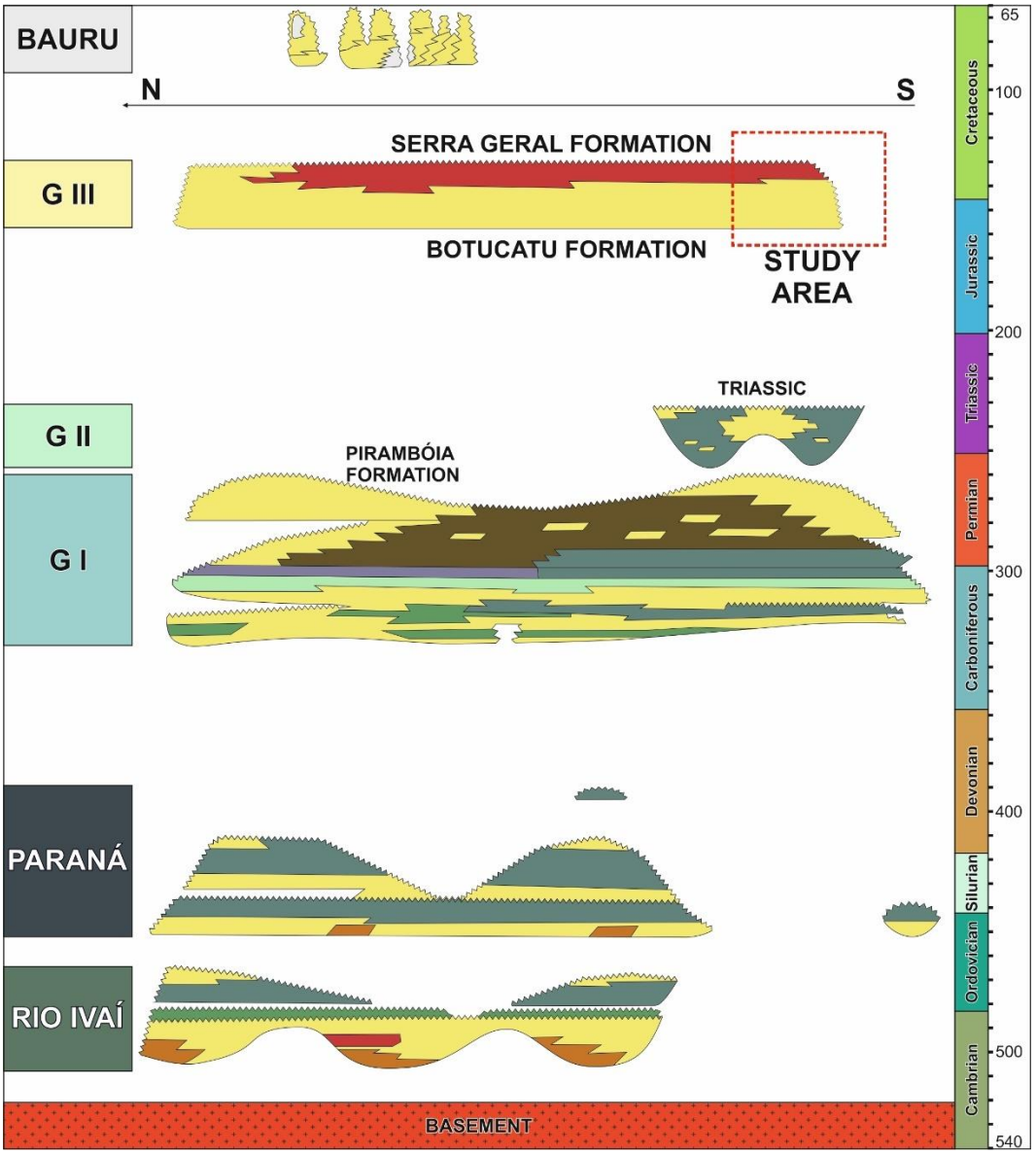

Figure 2 - Paraná Basin stratigraphic chart with the 6 Supersequences: Rio Ivaí, Paraná, Gondwana I, Gondwana II, Gondwana III, Bauru (Milani, 2007).

The study area is located along the southern margin of the Paraná Basin, in Rio Grande do Sul State (Brazil) and Central Uruguay. In Uruguay, the Botucatu

Formation is equivalent to the Rivera Member of the Tacuarembó Formation (Amarante *et al.*, 2019). The Botucatu Formation also has equivalent units in Argentina (San Cristobal Formation), Paraguay (Missiones Formation), Bolivia (Ichoa Formation) and Namibia (Twyfelfontain Formation) (Scherer and Goldberg, 2007). Outcrops in Rio Grande do Sul State and Uruguay likely represent the upwind margin of the erg as illustrated by: (i) variations in thickness from 0 to 100 m along the southern margin to up to 400 m thickness in the basin center (Milani *et al.*,1998), and (ii) paleocurrent data demonstrating a consistent NE/E paleowind direction along the southern basin margin (Scherer and Goldberg, 2007; Fig. 29).

Scherer (2000) described 4 facies across the southern Botucatu margin: thick large-scale trough cross-stratification; large-scale planar cross-stratification; medium-scale trough cross-stratification and low-angle cross-stratification. The relatively monotonous and simple sedimentary facies are controlled by dune morphology, illustrating a consistent predominance of crescentic dunes and linear draa bedforms. The Botucatu is considered to represent a dry-aeolian system (*sensu* Havholm and Kocurek, 1994), indicated by the absence of deposits or sedimentary features such as wet interdune deposits or adhesion structures generated by water-table or flooded/wet interdune areas.

In the study area, the Botucatu Formation overlies 3 distinct units of the Gondwana I and II supersequences of the Paraná Basin-fill: (i) the Jurassic Guará Formation and Batovi Member of Tacuarembo Formation (Uruguay) in the west; (ii) the Triassic Caturrita Formation in the central region and (iii) the Permian to Jurassic Pirambóia Formation in the east. The Guará Formation (Batovi Member) is an Upper Jurassic fluvial-aeolian unit, comprising a S-SW directed distributive fluvial system and small to medium size dunes (Scherer and Lavina, 2006; Amarante *et al.*, 2019). The

Triassic Caturrita Formation comprises amalgamated sandstones intercalated with siltstones that represent high energy, low sinuosity river deposits (Zerfass *et al.*, 2003; Jenisch *et al.,* 2017). The Permian Pirambóia Formation is a wet aeolian system, composed of red fine-to coarse sandstones (Dias and Scherer, 2008).

The Paraná Basin basement framework comprises a series of complex Cambrian to Paleoproterozoic rocks forming the following terranes (from East to West): Dom Feliciano Belt, Tacuarambó Terrane (Sul-Rio-Grandense Shield), Nico Pérez and Piedras Altas Terranes (Uruguayan Shield). For simplification, the overall crustal framework displays a distribution of Neoproterozoic ages in the East (Dom Feliciano Belt) and Paleoproterozoic age terranes in the West (Tacuarembó, Nico Pérez and Tacurambó Terranes) (Fig. 39). The Dom Feliciano Belt forms part of the Central-to-East Rio-Grandense Shield and includes 3 main orogenic events: Passinho (0.9 – 0.86 Ga), São Gabriel (0.77 – 0.68 Ga) and Dom Feliciano (0.65 – 0.54 Ga) (Philip *et al.*, 2016). Additionally, the Dom Feliciano terrane includes a Neoproterozoic-Cambrian volcano-sedimentary succession (Camaqua Basin) and a Neoproterozoic metamorphic syn-collision belt (Porongos Belt) (Höfig *et al.*, 2018; Janikian *et al.*, 2012). The granitic-gneissic Tacuarembó, Piedras Altas and Nico Perez Terranes are located on the Western Sul-Rio-Grandense and Uruguayan Shields. These terranes yield Orosirian to Archean ages, with peaks from 1.8 to 2.2 Ga (Oyhantçabal *et al.*, 2018a and 2018b).

3. Materials and Methods

To constrain the provenance of the Botucatu sandstones in the southwestern part of the Paraná Basin, sedimentary petrography, heavy mineral analysis, grain size analysis and detrital zircon geochronology were undertaken. Twenty-one samples

(Fig. 29) were collected along the southern margin of the basin from sandstones at the base and top of the formation together with sandstones from within the Serra Geral Formation lavas (Intratrap sandstones) to observe possible lateral and chronological changes in provenance signal. In the studied area, the Botucatu Formation outcrop ranges from 0.5 to 30 m in thickness and mostly comprises fine to medium sand. The predominant sedimentary facies are large-scale cross-beds, with occasional low-angle-beds, trough cross-bed sets and locally massive sandstones. Scherer (2000) considered these facies to represent parts of aeolian dune morphologies (simple to compound crescentic dunes and complex linear *draas*) with very local ephemeral fluvial stream deposits. Table 3 documents the sedimentary facies as well as the sample number, location, stratigraphic level (base, top and interbedded), and the provenance techniques performed. The samples were collected mostly form large scale cross- and trough-stratified sandstones (Ste), with some from low-angle stratified (Sle) and massive sandstones (Sm). Figure 31 shows the 11 studied profiles (based on Scherer, 2000) and the position of each sample within the stratigraphy.

Table 1 - Sample locations by stratigraphic position and location. Heavy Mineral (HM); Bulk Petrography (BP); Detrital Zircon (DZ); Granulometric Analysis (GR).

Sample Code	Facies Code	Stratigraphic Level	Coordinates Lat/Long	Region Sampled	Provenance Techniques			
					BP	DZ	HM	GR
PB-01	Sle	Base	-50.482903/-29.886139	East	X			
PB-02A	Ste	Top	-50.395787/-29.877412	East	X	X	X	X
PB-02C	Sm	Intratrap	-50.395787/-29.877412	East	X	X		
PB-03	Ste	Top	-50.529168/-29.830188	East	X			
PB-09	Ste	Top	-50.577807/-29.743651	East	X		X	X
PB-18	Ste	Top	-52.414231/-29.726391	East	X	X	X	X
PB-31B	Ste	Intratrap	-51.131414/-29.632367	East		X	X	X
PB-19	Sm	Intratrap	-52.634681/-29.55371	Central	X			
PB-20	Sm	Intratrap	-52.638663/-29.261931	Central	X		X	X
PB-21	Ste	Top	-52.631227/-29.566123	Central	X		X	X
PB-22	Ste	Intratrap	-53.0209/-29.406328	Central	X	X	X	X
PB-23	Ste	Base	-54.68608/-29.481004	Central	X	X	X	X
PB-24	Ste	Top	-54.749004/-29.365739	Central		X	X	X
PB-29	Ste	Intratrap	-54.764559/-29.36278	Centra	X			
PB-04	Sm	Base	-55.412019/-30.717301	West	X		X	X
PB-10	Ste	Base	-55.72246/-31.564436	West	X	X	X	X
PB-11	Ste	Top	-55.897349/-31.147843	West		X	X	X
PB-12	Ste	Intratrap	-55.913833/-31.142028	West		X	X	X
PB-14	Sle	Top	-56.216685/-30.486345	West			X	X
PB-16	Ste	Top	-55.517067/-30.852035	West	X			
PB-17	Ste	Base	-55.349101/-30.82337	West	X			

Sample preparation was undertaken separately for each analysis. For granulometric and heavy mineral analysis, disaggregation was carefully undertaken with a rubber point pestle and mortar to avoid grain breakage. For geochronological studies sample disaggregation was carried out using a mechanical jaw crusher (when necessary) and a plate mill.

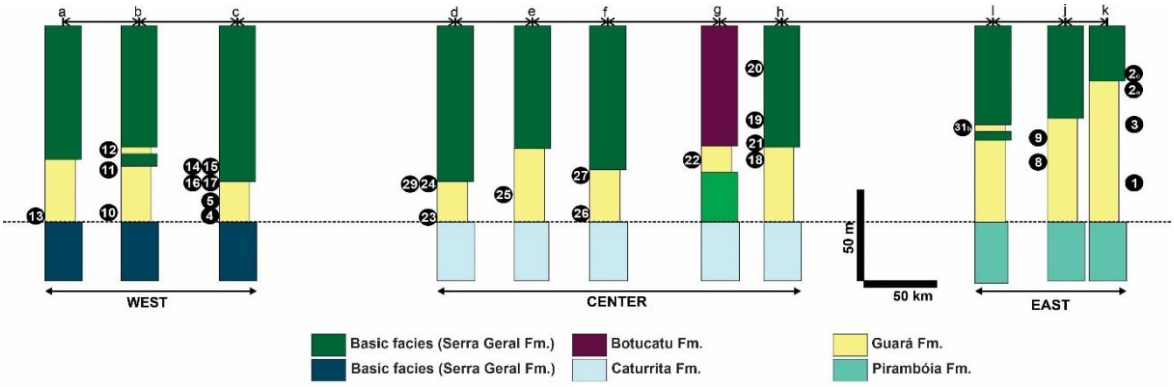

Figure 3 - Sedimentary profiles (Adapted from Scherer 2000) with the stratigraphic position of the sampling where the leters a-k refers to the profile locations a- Tacuarembó (Uy); b- Tranqueras (Uy); c- Santana do Livramento (Br); d- Jaguari (Br); e- Sao Pedro do Sul (Br); f- Santa Maria (Br); g- Sobradinho (Br); h- Herveiras (Br); i- Ivoti (Br); j- Santo Antônio da Patrulha (Br); k- Osório (Br)

Nineteen petrographic thin sections were described and subject to point counting (300 points/sample) using the Gazzi and Dickinson method (Ingersoll *et al.,*1984). The results are displayed following the scheme of Garzanti (2018) (Fig. 32).

Grain size analyses were undertaken on fourteen samples, with 100g of each sandstone. The process consisted of sample cleaning (removal of external exposed surfaces), disaggregation, drying and sieving. The petrographic data reveal no silt sized grain-size, justifying the sand-class interval measuring (63-125 μm, 125-250 μm, 250-500 μm, 500-1000 μm). Samples were weighed after each step and the difference recalculated and assigned to each respective grain size proportion.

Between 150 to 400g of fourteen samples were selected for heavy mineral analysis. Samples were dried and sieved (63-125 μm) following the grain-size window interval of Morton and Hallsworth (1994) via dense liquid separation (Bromoform -2.80 g/mL). The mainly fine sand sediment framework composition of the Botucatu Formation is compatible with hydraulic equivalence of heavy mineral assemblage, ruling out significant hydraulic sorting bias effects (e.g. Morton and Hallsworth, 1994; Hurst *et al.*, 2017).

Heavy mineral concentrates were mounted on petrographic slides, with identification of 150 translucent minerals using the ribbon technique following the method of Mange and Maurer (2012). A complementary elemental analysis was undertaken with an energy-dispersive X-ray spectrometer (EDS) on a scanning electron microscope (SEM) to aid with heavy mineral identification. The analysis was carried out at the Universidade Federal do Rio Grande do Sul using a Jeol 6610-LV (15 kV beam voltage and 12mm working distance).

Detrital zircon grains were analyzed from 10 samples for U-Pb at University of São Paulo, using a Finnigan Neptune mass spectrometer and an excimer ArF laser (λ=193nm) ablation system. The laser ablation multi-collector inductively coupled plasma mass spectrometry (LA-MC-ICP-MS) uses 5 mJ, 6 Hz and 29 μm diameter beam as analytical conditions. The $^{207}Pb/^{206}Pb$ ages were used for zircons older than 1.3 Ga and the $^{206}Pb/^{238}U$ ages for younger grains. The discordance tolerance is 10%, values above this limit were dismissed. The parameters used are discussed in Sato *et al.* (2011).

The GRADISTAT software (Blott and Pye, 2001) was used for statistical analysis and to determine sediment distribution. The Provenance R Package (Vermeesch *et al.,* 2016) was used to run the cumulative age densities (CAD), kernel densities estimators and Multidimensional Scaling (MDS) plots.

4. Results

Petrography reveals a mean composition of $Qt_{89}F_8L_3$, compositionally classified (Garzanti, 2018) as pure-quartzose (PB-04, -23), quartzose (PB-01, -03, -10, -16, -17, -18, -19, -21, -22, -24, -29A) and quartz-rich feldspatho-quartzose (PB-2A, -2C, -09, -20) (Fig. 32) sandstones. Monocrystalline quartz is predominant (93 to 100%) over

polycrystalline quartz. K-feldspar is most frequent over plagioclase (mean 70%), however center region samples show an increase in plagioclase (60 to 70%). The lithic fragment distribution (Fig. 32B) shows both igneous (felsic plutonic) and volcanic (basaltic lathwork to glassy trachyte) fragments. In the eastern and central regions moderately sorted fine sand predominates with poorly sorted medium sand in the west.

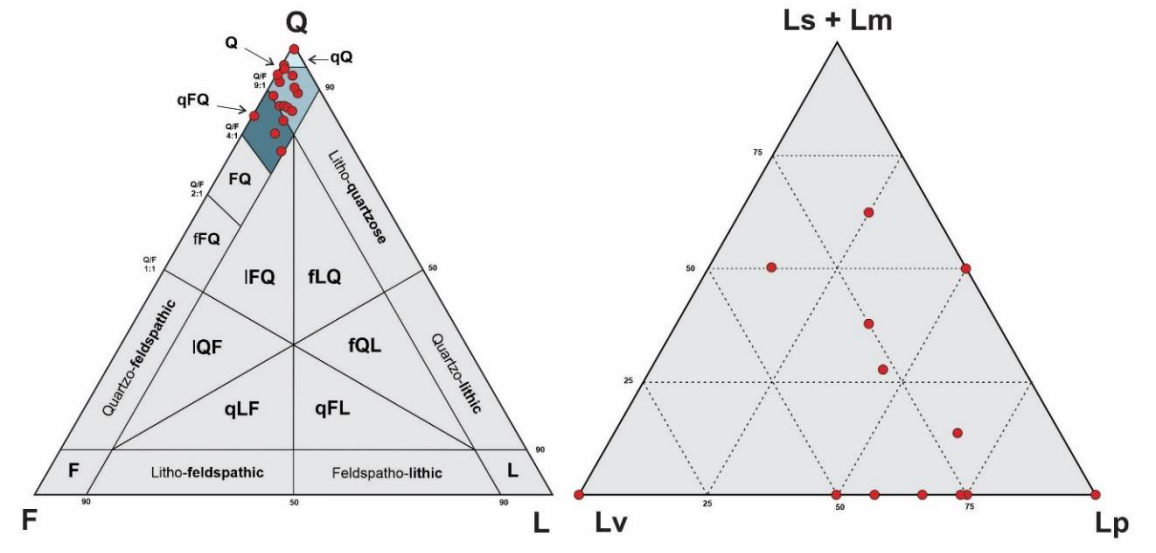

Figure 4 - Sandstones classification scheme (Garzanti 2018) and lithics plot. Samples point to quartzose and felsic plutonic compositions. (Q- Total quartz; F – K-feldspar and plagioclase; L- total lithics; Lv- volcanic rock fragments; Lp – Plutonic lithics; Lm and Ls- metamorphic and sedimentary lithics; qQ- pure-quartzose; Q- Quartzose; qFQ- quartz-rich feldspatho-Quartzose).

The heavy mineral population of the 21 studied samples comprises 14 mineral species, with a dominant signal from resistant species - zircon, rutile, and tourmaline. Local occurrences of anomalously high amounts of garnet, epidote, pyrolusite and apatite and a few grains of other species such as alumino-silicates (kyanite, andalusite or sillimanite), spinel, corundum, monazite, fluorite, xenotime, sulfides (cassiterite and pyrite) are also recorded. Figure 333 shows the heavy mineral assemblage distribution across the studied region, illustrating the high ZTR and very-local occurrences of garnet, epidote and pyrolusite. The heavy mineral analysis presents a mean $ZTR_{0.84}$, ranging from 33.5-to 99.4% and is characterized by the predominance of zircon,

reaching almost 98% in sample PB-24. The area contains zircons that display different levels of roundness, varying from rounded oval grains to elongate bi-pyramidal prismatic grains. Samples PB-2A, -31B, -20 show peaks in Fe-garnet and epidote and sample PB-09 contains a high abundance of pyrolusite.

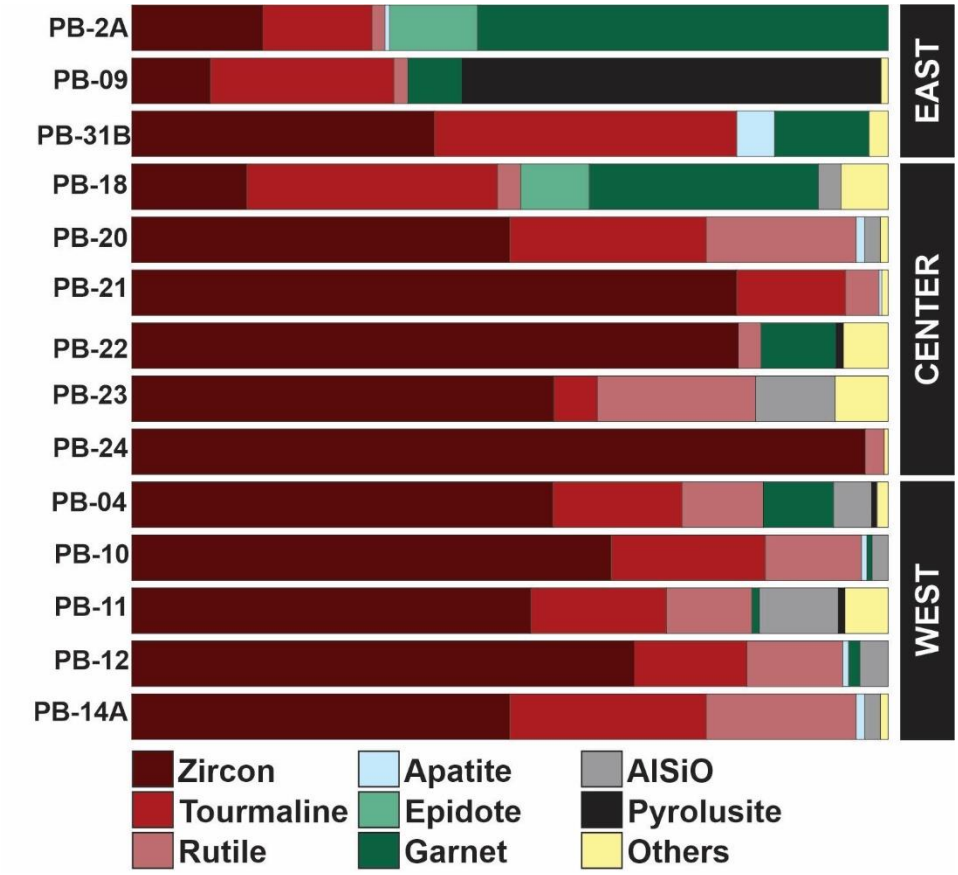

Figure 5 - Heavy mineral suites distribution across the regions, with prevalent zircon, tourmaline and rutile (ZTR) assemblage.

Detrital zircon age spectra display a complex signature, with ages ranging from 155 Ma to 3290 Ma. The wide age distribution reflects the complex geologic history of the basement rocks and potential recycling from older sedimentary units. In order to track possible sediment pathways using the detrital zircon (DZ) record, the ages were separated into 7 groups that correspond to significant crustal construction periods in South America (Bahlburg *et al.,* 2009): Late Paleozoic to Mesozoic (Gondwanides Cycle), Devonian to Cambrian (Famatian Cycle), Cambrian to Neoproterozoic

(Brasiliano/ Pampean/ Pan-African cycles), Tonian to Stenian (Grenvilian Cycle), Mid-Mesoproterozoic to Statherian, Orosirian to Rhyacian and Neo- to Paleoarchean (Fig. 33).

The detrital zircon data indicate that Early Neoproterozoic to Cambrian ages (515-650 Ma) are the main contributor to the DZ population with Late Paleozoic to Mid Mesozoic (150-359 Ma), Tonian-Stenian (0.9 – 1.25 Ga) and Orosirian to Rhyiacian ages (1.8- 2.25 Ga) forming subsidiary contributions. The detrital zircon signal appears to be relatively homogeneous but grouping the samples by region reveals a transitional signature across the southern margin of the Botucatu desert, with increasing Cambrian to Neoproterozoic ages (31.6 to 52.5%) and a decrease in ages older than 900 Ma towards the East.

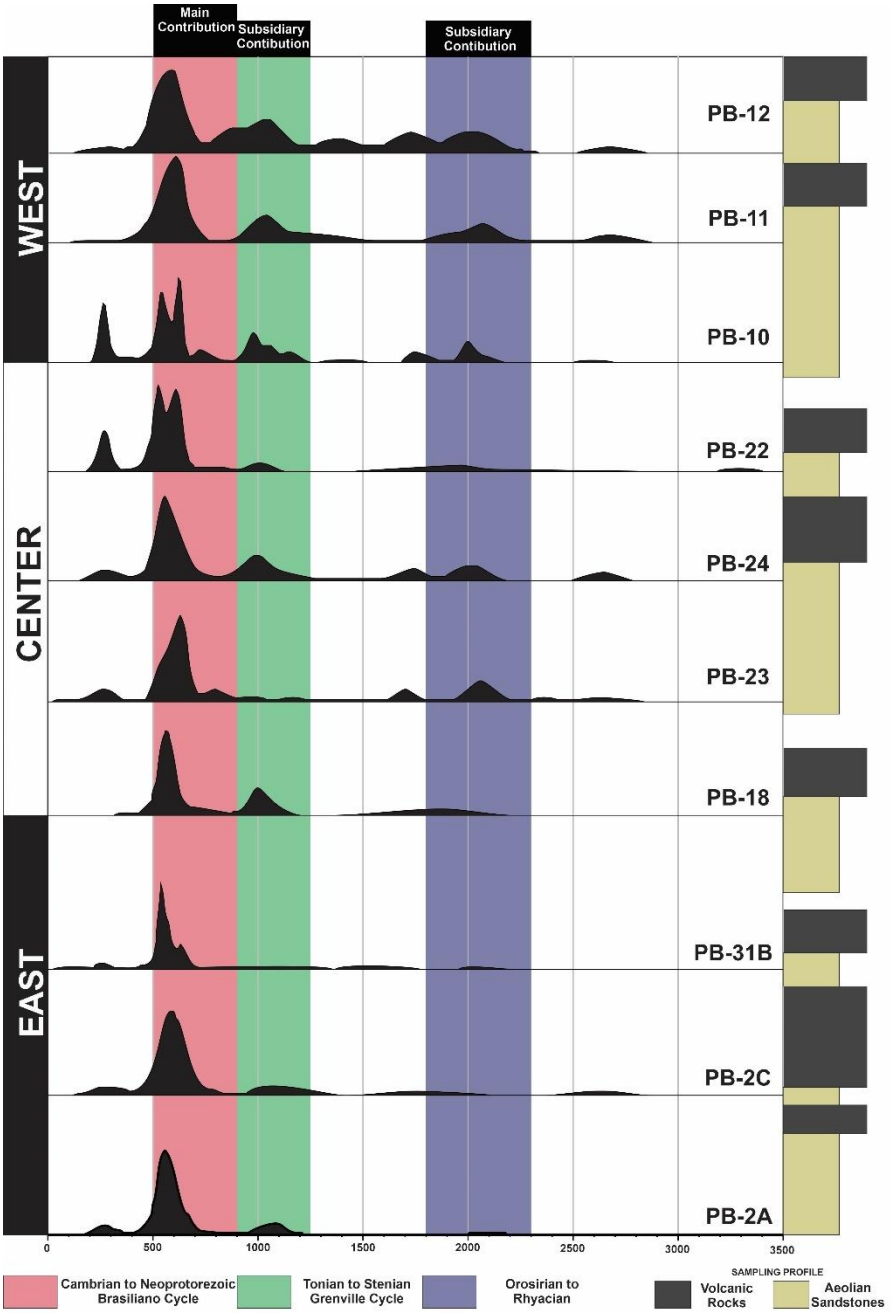

Figure 6 - Normalized probability density plots located on the schematic stratigraphic profile. The colored areas demonstrate the most prominent age intervals.

The geographic location of each sample and a compilation of the different dataset types are illustrated in Figure 35. U-Pb detrital zircon ages are plotted using a probability density plot, the bulk petrography, heavy mineral, and granulometric analyses are illustrated using pie charts. The sampling level in the stratigraphy and

location relative to the Serra Geral lavas are also shown in Figure 31. The provenance dataset reveals a lateral variation described in further detail below.

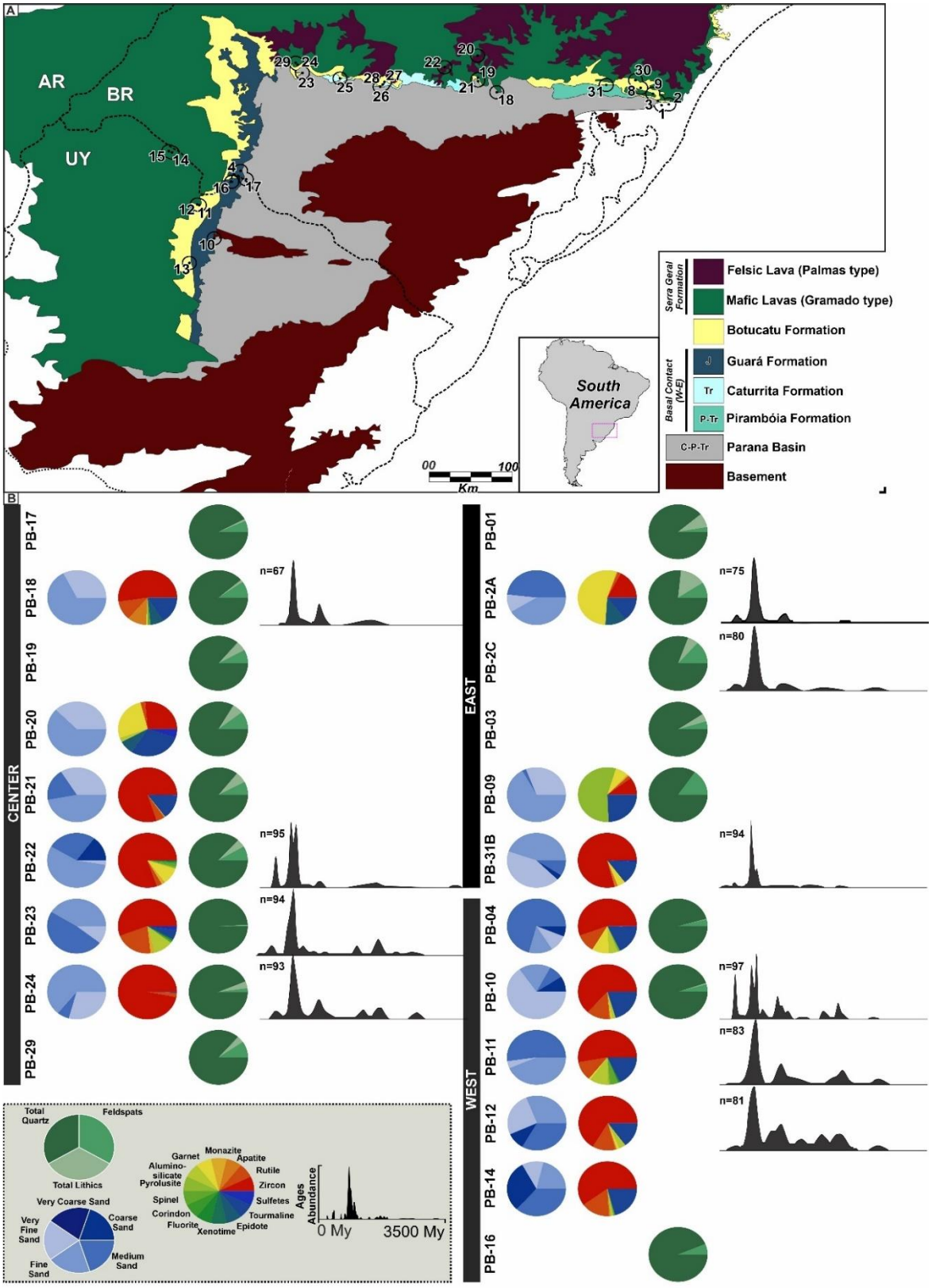

Figure 7- Geologic map (adapted from Wildner et al. 2006) with the sampling spots; B - Provenance data compilation.

4.1 Eastern Region

Three sections were sampled in the eastern region: Santo Antônio da Patrulha (PB-03 and -09), Osório (PB-01, -02A, -02C) and Ivoti (PB-31B) (see Figure 31). Bulk petrography shows a mean composition of $Qt_{85}F_{11}L_4$, with a relative change in feldspar content (5 to 15%). The granulometric analysis reveals a unimodal distribution, fine-sand, moderately (PB-02A, PB-31B) to moderately well sorted (PB-09). The heavy mineral analyses (Fig. 33) revealed that samples PB-02A and -31B contain 54.3% and 12.5% of almandine respectively, PB-02A contains 11.5% epidote and sample PB-20 comprises 55.4% pyrolusite. Detrital zircon dating reveals an age signature ranging for 155 Ma to 3231 Ma, with main peaks in the Late Paleozoic to Mid Mesozoic (11%), Neoproterozoic to Cambrian (52%) and Tonian to Stenian (10%). Eastern region samples show a significant upward increase in the proportion of C-NP zircons from 49% at the base (PB-02A) to 72% in interbedded sandstones (PB-31B) at the top of the Botucatu Formation.

4.2 Central Region

The central portion samples were collected from 5 sections (Fig. 31): Jaguari (PB-23, -24, -23), Sao Pedro do Sul (PB-25), Santa Maria (PB-26, -27), Sobradinho (PB-22) and Herveiras (PB-18, -21, -19, -20). Petrography reveals a mean composition of $Qt_{89}F_7L_3$, classified as quartz-enriched feldspatho-quartzose and quartzose sandstones. Bulk petrography shows total quartz varying from 83 to 99%, feldspars from 0 to 10% and total lithics from 0 to 6%. Grain-size analysis reveals a unimodal distribution, moderately well (PB-18, -20, -24) to moderately sorted (PB-21, -22, -23), fine-sand to medium-sand (PB-23). Heavy mineral analysis (Fig. 33) shows

a variable ZTR value, ranging from 51.5 to 99.5%, with a garnet peak (30.3%) occurring in sample PB-20. Samples 18, 21, 22, 23 and 24 have high zircon, tourmaline and rutile (ZTR) values, reaching >95% zircon in sample 24. Fe- garnet and epidote are observed in sample 20 (>35%). Detrital zircon ages range from 174 Ma to 3290 Ma, including Early Neoproterozoic to Cambrian (41 %), Tonian - Stenian (12 %) and Orosirian-Rhyacian (10%) peaks.

4.3 Western Region

Seven samples were taken from the western part of the study area from 3 sections (Fig. 31): Tacurambó (PB-13), Tranqueras (PB-10, -11, -12) and Santana do Livramento (PB- 4, -5, -14, -15, -16, -17) in Uruguay and Brazil. Petrographically the samples have a predominantly quartzose composition (mean $Qt_{94}F_5L_0$). The granulometric analysis shows unimodal sorting, moderate-well (PB-11), moderately (PB-04, -10) to poorly sorted (PB-12, -14A), medium- (PB-04, -11, -14A) to fine sand (PB-10, -12).). Heavy mineral analysis (Fig. 33) reveals high ZTR concentration (83 to 96%) with zircons dominant. The region has a higher than average rutile content (13%) contrasting with a mean of 5% from other regions. Al-Si polymorphs (mean 5%) appear consistently in the west but only occur occasionally in the east and central regions. Garnet (Fe-Almandine) appears only in sample PB-04. Detrital zircon grains from samples PB-10, PB-11, and PB-12 display ages ranging from 155 Ma to 2717 Ma, with mainly Early Neoproterozoic to Cambrian (32%), Tonian to Stenian (18%) and Orosirian to Rhyacian (14%) peaks.

5. Discussion

5.1 Lateral variations

The detrital zircon geochronology dataset illustrates that Cambrian-Neoproterozoic (C-NP) aged zircons form the main component of the population with the Tonian-Stenian (0.9-1.25 Ga) and Orosirian-Rhyacian (1.80-2.25 Ga) providing subsidiary contributions in all regions. More detailed analysis allows lateral variations in age groups can be distinguished. Variations in detrital zircon age distributions across the regions are compiled in Table 4 and demonstrate a relative increase in C-NP ages in the eastern region, with a predominance of >900 Ma grains in the western region. The central region is transitional between both regions containing intermediate values in all age periods.

Table 2 - Detrital zircon age proportions from the southern margin of the Botucatu Fm. organized by regions. The data show an overall increase in>900 Ma ages to the west and Brasiliano peak to the east.

Event	Time Interval (Ga)	%		
		East	Center	West
Late Paleozoic to Mid Mesozoic	0.150-0.359	11.027	9.695	9.294
Early Famatian (Ordovician-Silurian)	0.359-0.515	8.365	6.648	5.948
Early Neoproterozoic to Cambrian Ages (Late Brasiliano)	0.515-0.650	52.471	40.720	31.599
Early Brasiliano	0.650-0.900	9.886	9.418	7.807
Tonian-Stenian Ages (Grenvillian Cycle)	0.900-1.250	9.886	11.634	18.216
Mid-Mesoproterozoic to Statherian ages	1.250-1.800	3.422	6.648	9.665
Orosirian to Rhyacian ages	1.800-2.200	2.662	9.695	12.639
Neo- to Paleoarchean	2.200-3.400	2.281	5.540	4.833

The lateral variations described above are likely to be related to changes in either basement units immediately adjacent to the outcrop or to recycling of underlying sedimentary successions or a combination of both. These variations are also expressed in Figure 36 as cumulative density plots (A) and multidimensional scaling

plots (B). The CDP demonstrates that the C-NP is the most variable detrital zircon age group from east to west, with almost 20% variation, whilst the MDS plots illustrate the transitional characteristics of the lateral changes. The average compositional dataset (granulometry, petrography and heavy minerals) also displays a lateral modification from West to East. The petrography shows an increase of lithics and feldspar over quartz components ($Q_{94\text{-}5}F_{5\text{-}10}L_{0\text{-}5}$), and the granulometry demonstrates a medium to very fine sand transition. The heavy mineral data presents an increase of the mean ZTR from 80 to 89% (East to West). The western region also shows an increase of Al-Si minerals, suggesting greater influence of metamorphic sources.

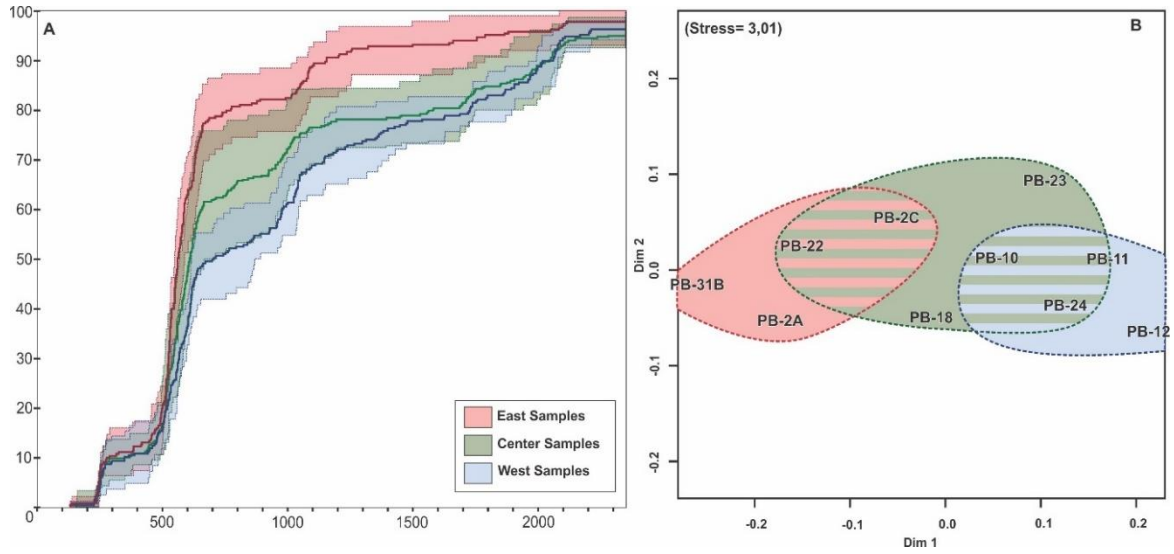

Figure 8 - Cumulative probability plot (A) and MDS plots (B) illustrating the lateral variability of detrital zircon U-Pb ages. Western region is enriched in older ages (>1.25 Ga) whilst the eastern region isdominated by Early Brasiliano ages (515-620 Ma). The central portion of the basin is transitional between the two. The bold central lines in plot A correspond to the sum of values for each region.

In the study area, the Paraná Basin is developed above a basement composed of Neoarchean to Cambrian rocks. The contact between basement and basin-fill occurs beneath Permian units (Itararé and Rio Bonito Formations), as such there is no direct contact between basement and the Botucatu Formation. In addition, the basal contact of the Botucatu changes laterally, from the Upper Jurassic Guará Formation/ Rivera Member (West), Triassic Caturrita Formation (Central) and Permian

Pirambóia Formation (East). No detrital zircon age data are available from these underlying units, so it is not possible to ascertain if zircons were derived directly from these strata. Zircon ages from the underlying basement also show distinct age domains across the margin. The Rio-Grandense and Uruguayan Shields, contain zircon populations of 500 – 900 Ma (Cambrian- Neoproterozoic contribution) and 1250-3400 Ma (including Orosirian-Rhiacian subsidiary contribution) (Philip *et al.,* 2016). Tectonic domains such as the Piedras Altas, Nico Pérez and Tacuarembó terranes, yielded multiple Neoproterozoic to Neoarchean ages, but overall ages are composed predominantly of >1.25 Ga rocks (Oyhantçabal *et al.,* 2012; Santos *et al.,* 2003; Oriolo *et al.,* 2016). The Dom Feliciano Belt in Rio Grande do Sul State and the coastal region of Uruguay comprises a Cambrian to Neoproterozoic granite-gneissic orogenic belt (Philip *et al.,* 2016, Basei *et al.,* 2008). The progressive upward increase in C-NP ages in the Eastern region (48.8% to 71.6%) could indicate increased direct input from these source terrains at this location.

A lack of direct first cycle input into the majority of the Botacatu Formation is indicated by the limited presence of detrital zircon grains of Jurassic age (180-155 Ma). These grains occur only in the extreme west of the Botucatu exposure (Central Argentina) where they are considered to be derived directly from the Andean magmatic arc (Peri et al. 2016). The Tonian-Stenian ages (Grenvilian Cycle) are not present in basement terranes close to the study area and could indicate an original source in areas such as the Sierra Pampeanas (Argentina) and Natal-Namaqua Belt (SW Africa) (Rapela *et al.,* 2010; Casquet *et al.,* 2008; Bial *et al.,* 2015).The relative increase in zircons derived from strata that yielded Tonian-Stenian ages in the western region together with the prevailing NE wind pattern could indicate that first-cycle grains were derived from the SW Gondwana margin terranes (Sierra Pampeanas). Canile *et*

al. (2016) show that juvenile zircons (Positive ƐHf) from the Natal-Namaqua belt (in present day Namibia and South Africa) are present in older Paraná Basin units, demonstrating the existence of previous recycling. The Tonian-Stenian age signature probably records the presence of recycled grains from a mixture of Natal-Namaqua Belt and Western Sierra Pampeanas sources.

5.2 Sedimentary Recycling

U-Pb detrital zircon dating is a useful tool that allows the resulting age spectra from a sedimentary rock to be linked potentially to an original sediment source (Gehrels, 2014). However, due to the resistance of zircon to transport, burial and even metamorphic events, detrital zircon age spectra commonly include grains recycled from older strata such that the final detrital zircon age spectra within a sedimentary rock represent a composite of original and recycled material (Dickinson and Gehrels, 2009; Hadlari *et al.*, 2015). As a consequence, if solely utilizing the detrital zircon dataset it is a virtually impossible to establish if the age peaks in the Botucatu are derived directly from basement (1st cycle sediment) or by multiple phases of deposition and reworking (poly-cycling sediment). By combining the detrital zircon data with petrographic and heavy mineral data it is possible to more precisely determine the sediment origin. The petrographic and heavy mineral dataset shows a highly quartzose and ZTR-rich composition. A quartzose sedimentary factory requires multiple steps of diagenesis, weathering and recycling in order to obtain a pure-quartzose and high ZTR end-member (e.g Congo River sediment described by Garzanti *et al.*, (2019), suggesting that Botucatu sediment has a predominant poly-cyclic history. To understand the polycyclic sediment history of the Botucatu sediment and its relationship with Paraná Basin Carboniferous-Jurassic units, we compare the

detrital zircon data presented here, with other datasets from older strata in the southern Paraná Basin.

Cumulative age density and multidimensional scaling biplots (Figs 35A and B) are utilized to assess and compare the DZ populations present in the Carboniferous Itararé Group (Rio do Sul Fm.), Carboniferous-Permian Guatá (Palermo, Sideropólis, Paraguacu and Triunfo Fms.), Permian Passa Dois Group (Irati, Serra Alta, Teresina, Morro Pelado and Serrinha Fms.), Triassic Santa Maria formation (Santa Maria and Santa Catarina region- based on Canile *et al.*, 2016; Philip *et al.*, 2018). The MDS biplot (Fig. 37A) shows a distribution of units enriched in Paleoproterozoic sources (Rio Bonito and Palermo Formation), Permian-Triassic ages (Irati, Serra Alta, Teresina Formation), Cambrian-Neoproterozoic ages (Triassic and Eastern Botucatu) and a zone of mixed ages (Center, West, N Botucatu, Itararé, Serrinha, Triunfo Formations) can be defined. The MDS shows that the Late Carboniferous-Early Permian units (Rio Bonito and Palermo Formations) corresponds to a western Botucatu signature, suggesting that these units were the primary source.

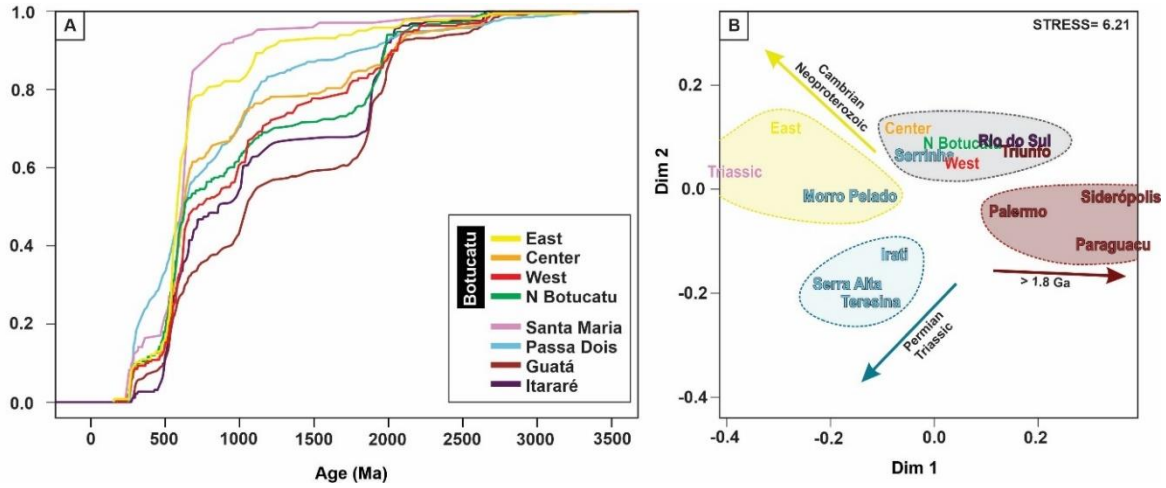

Figure 9 - Paraná Basin polycyclic nature revealed by CAD (A) and MDS plots (B), demonstrating an overlapping of detrital zircon ages from Carboniferous to Cretaceous strata (data from Canile et al., 2016; Phillip et al., 2018).

The conglomeratic end-member of the Triassic unit (Santa Cruz Sequence - Philip *et al.*, 2018) contains an assemblage enriched in Cambrian-Neoproterozoic ages, whilst finer grained components display a complex Permian to Paleoproterozoic age distribution. The similarity between the conglomerate end-members (Triassic) and eastern Botucatu samples (MDS and CAD) suggests that eastern Botucatu samples contain a relatively smaller amount of recycled material in comparison to central/west samples, especially in intratrap (PB-31B) samples.

ADD Jurassic grains.

5.3. Controls on Heavy Mineral Assemblages

The MDS biplot of the heavy mineral (Fig. 38) data defines two distinct clusters: (i) a well-defined group, referred to here as the average Botucatu composition and (ii) isolated samples referred to as local detrital component. The average Botucatu composition includes the majority of studied samples and has a mean composition of $ZTR_{0.9}$, with samples distributed throughout the basin, irrespective of stratigraphic level (basal, top or interbedded sandstone) or the sampling region (west, center or east). The local detrital component has a mean composition of $ZTR_{0.6}$ related primarily to peaks of Fe-Garnet, epidote, and Mn oxides (samples PB -31B, -20, -2A, -09). Fe-Garnet and epidote are common heavy mineral constituents, although pyrolusite is infrequent. Mn oxides are common in Serra Geral lavas, and its presence in the Botucatu indicates an authigenic phase. The heavy mineral and petrographic composition of the Botucatu Formation is considered to be representative of the original sediment source composition with little subsequent modification by burial diagenesis and weathering the reasons for which are discussed below.

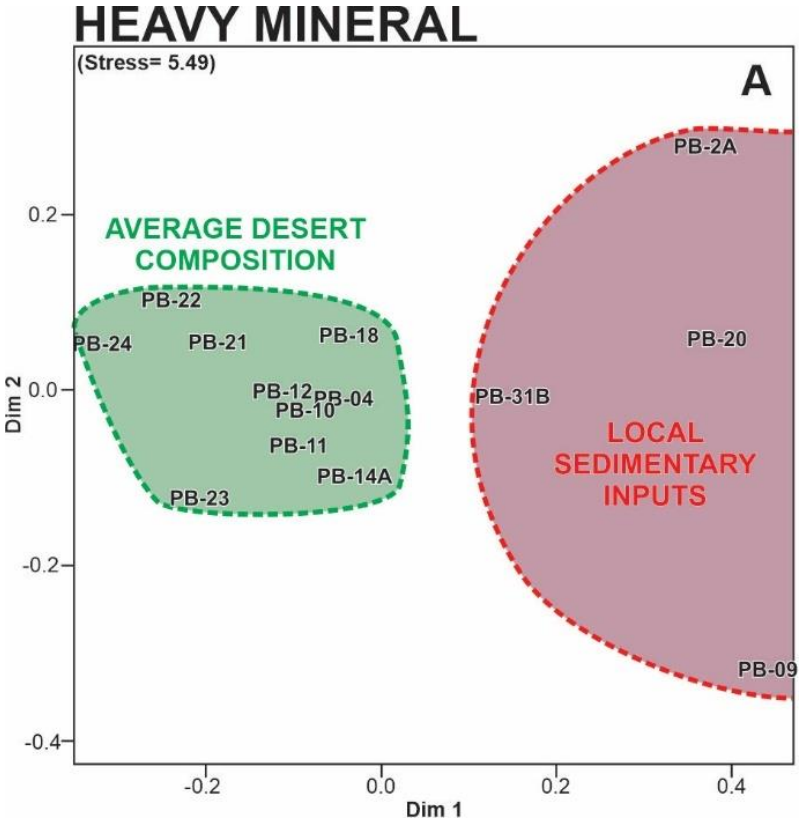

Figure 10 - MDS biplot on heavy mineral dataset demonstrates an average composition (ZTR-rich) and local detrital input (garnet, epidote and pyrolusite).

Morton and Halllsworth (2007) described the effects of burial related dissolution on heavy mineral assemblages. They demonstrated that epidote and garnet remain stable until respectively 1.0 and 3.5 km in the North Sea Basin. Andò (2012) in a study of cores from Bengal Bay showed that the progressive dissolution of amphibole occurred at burial depths of up to 1.5 km and for epidote at depths of up to 2.5 km, transitioning to a garnet and ZTR assemblage below 2.5. km depth. The Botucatu burial history suggests relatively shallow burial of up to 1.5 km in the basin depocenter in the north (Milani, 2007). The thinner lava-pile and absence of upper-basalt sedimentary deposits along the southern margin, points to a relatively shallower burial depth of 700-800 m (lava-pile thickness in south). Limited burial suggests that the presence of garnet and epidote is not controlled by burial related dissolution but likely due to provenance controls.

The common presence of micro- and moldic porosity (on lithics and feldspars) and feldspar dissolution may suggest a degree of surface weathering altering the composition on outcrops. However, França *et al.* (2003) describes feldspar dissolution in well cores, such that the process also occurs at depth. The sampling occurs mostly on road-side outcrops in similar climatic condition (humid and hot) across the studied area. If differential dissolution was the driving mechanism to generate local compositional variations, intermediate of heavy minerals assemblages would also be expected with highly weathered/dissolved garnet and epidotes in ZTR enriched samples, which does not occur. Thus, the local variations apparently are not controlled by differential surface weathering, indicating the heavy mineral and petrographic changes are depositional.

Reconstructions of desert depositional systems (e.g. Pye and Tsoar, 2008) illustrate the coexistence of different depositional environments such as rivers, alluvial fans and deltas that could provide sediment for a dune field. An erg margin, as in the study area, is prone to different styles of interaction between depositional systems, particularly at the fluvial-aeolian interface (Al-Masrahy and Mountney, 2015). Whilst there are very few preserved records of waterlain deposits in the dry-aeolian Botucatu system, fluvial input is likely to have occurred around the erg margins with subsequent aeolian reworking removing that sedimentary signature. Provenance studies from present day deserts such as Taklamakann (Rittner *et al.,* 2016), Arabia (Garzanti *et al.,* 2013) and Namibia (Garzanti *et al.,* 2012), demonstrate that shifts in provenance can be correlated with fluvial, alluvial fan or deltaic inputs. The localized heavy mineral peaks (Fig. 33) concomitant with increase in quartz content suggests a point-sourced alluvial system reworked laterally by aeolian processes. Aeolian systems promote an

increase in grain roundness, but at the same time maintain stable heavy mineral proportions (Resentini *et al.*, 2018).

6. Multiscale desert filling

Despite the similarities in the petrographic, heavy mineral and detrital zircon compositions, subtle differences are present in the dataset, indicating the presence of additional controls on sandstone composition. The data set reveals two important characteristics: (i) lateral variations in detrital zircon age spectra and (ii) differences in heavy mineral and petrographic data that suggest local sediment input points. The lateral provenance variations (5.1) are illustrated on Figure 39, demonstrating that the detrital zircon, granulometry, petrography and heavy mineral assemblages change from East to West. Additionally, the figure shows the underlying units (Paraná Basin) and basement terranes that compose the Sul-Rio-Grandense and Uruguayan shields.

As discussed in 5.2, the detrital zircon composition of Botucatu and Paraná Basin units display a statistical similarity, suggesting that underlying units provided the last sediment source for the Botucatu Desert. Figure 39 displays the overlap of the lateral variations and underlying units of Botucatu (Guará Fm., Santa Maria Fm., and Pirambóia Fm.) suggesting these units as the most feasible sediment source. Furthermore, Figure 39 illustrates how ultimately the basement age framework contributes to the lateral detrital zircon variation. The prevalent >900 Ma terranes in the West (Tacuarembó, Nico Perez and Piedras Altas) contrasting with the C-Np ages at East (Dom Feliciano Belt) probably contributed with Ordovician to Jurassic Paraná Basin filling, later being rework for Botucatu. The grain-size, heavy mineral and petrography partly support the lateral changes in the detrital zircon population, supporting the notion that reworking of Paraná underlying rocks was the main reason

for the lateral variation. The large-scale control (up to 600km margin) shows that aeolian processes were not able to completely homogenize the overall composition of the sand supplied to the Botucatu erg.

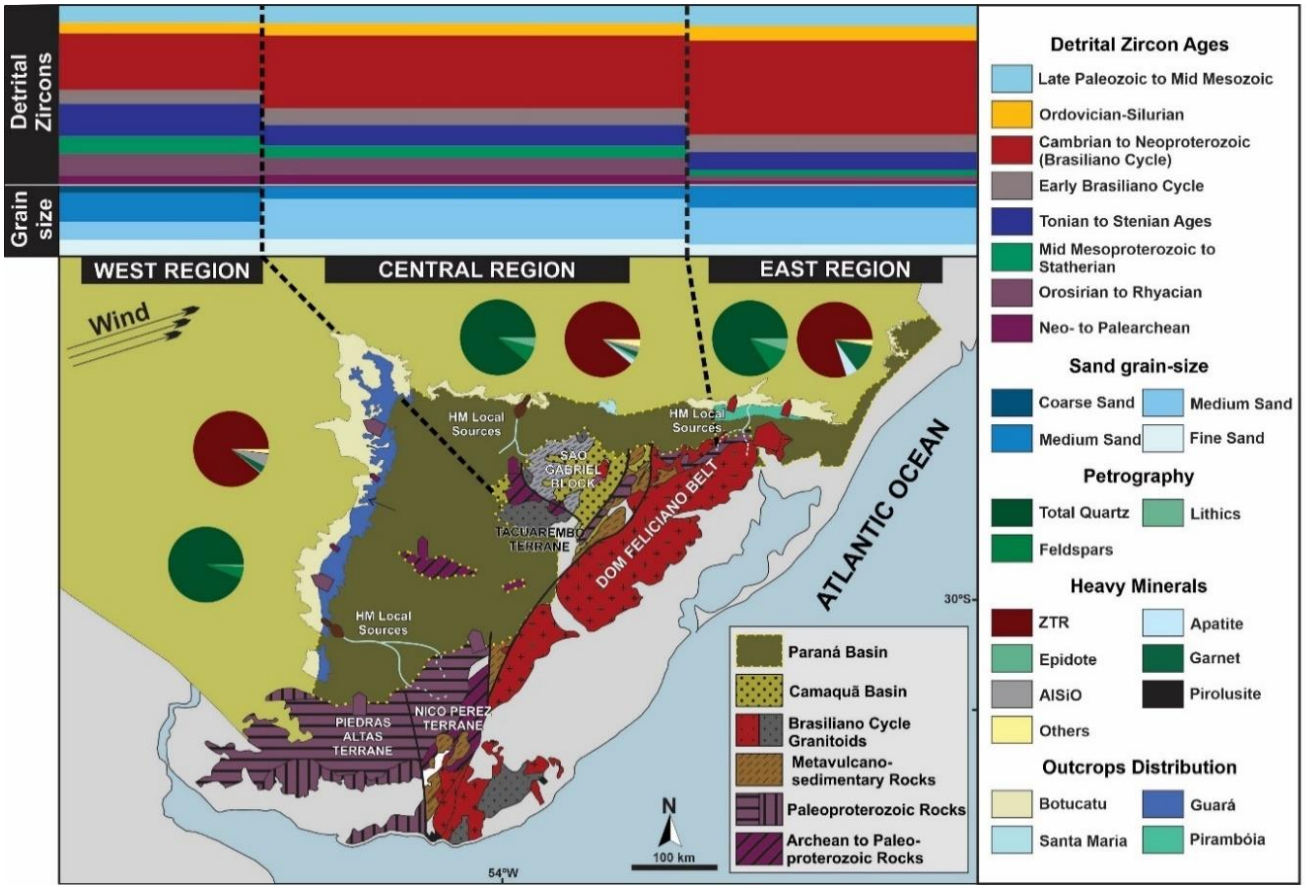

Figure 11 - Source-to-sink map demonstrating the impact of surrounding basement and external sources on the Botucatu DZ composition. Pie-charts displays the mean petrography and heavy mineral compositions, mirroring a lateral variation with DZ and granulometric data. At local level, fluvial inputs generate heavy mineral anomalous compositions. Data for the basement are from Saalman *et al.* (2011) and the desert extent is from Scherer and Goldberg (2007)

The anomalous heavy mineral values characterize local sedimentary input, however, is not clear if this input was sourced directly from basement material, reworked from older, underlying sedimentary successions or combination of both. Figure 39 illustrates the fluvial systems draining Paraná Basin units and possible basement terranes. The evidence for local sediment input supports the idea of a

number of distinct sediment pathways into the Botucatu erg, resulting in distinct, identifiable compositional signatures.

7. Conclusions

A provenance analysis of the aeolian sediments of the Botucatu Formation along the southern margin of the Paraná Basin has been undertaken to provide insights into depositional controls. The provenance dataset of detrital zircon U-Pb dating, heavy mineral analysis, petrography and granulometric analysis using multi-statistical tools (multidimensional scaling, cumulative density plot, and density plots) indicate that:

- Cambrian to Neoproterozoic ages (515-650 Ma) are the main detrital zircon component, with subsidiary contributions from Orosirian to Rhyacian (1.8-2.2 Ga) and Tonian to Stenian ages (0.9-0.125 Ga);

- A progressive lateral change in detrital zircon ages together with changes in the underlying basin stratigraphy and basement domains suggests a polycyclic provenance;

- Eastern region records an upward increase of Cambrian to Neoproterozoic detrital zircons, central and western regions show no significant changes;

- There is a progressive downwind decrease in grain size from medium to very fine sand over a distance of 600 km from downwind;

- An average quartz-ZTR enriched composition predominates along the southern Botucatu margin, variations allow recognition of local sediment input points within an otherwise homogenous aeolian system which likely relate to local fluvial systems developed along the erg margin.

8. Acknowledgments

The authors gratefully acknowledge support from Shell Brasil through the 'BG05: UoA-UFRGS-SWB Sedimentary Basins' project at UFRGS and the strategic importance given by ANP through the R&D levy regulation. The authors would like to thank Renan Guilherme de Souza and Adriano Reis for help in Tacuarembó/Uy Field Trip. This work is part of the current dual-degree Ph.D. from Gabriel Bertolini at Universidade Federal do Rio Grande do Sul and University of Aberdeen. We thank to Conselho Nacional de Desenvolvimento Cientifico e Tecnológico (CNPq) by the financial support (Grant: 203786/2017-3).

9. References

Al-Masrahy, M. A. and Mountney, N. P. (2015) A classification scheme for fluvial-aeolian system interaction in desert-margin settings. *Aeolian Research*, 17, 67-88.

Amarante, F. B., Scherer, C. M. S., Aguilar C. A. G., Reis, A. D., Mesa, V. and Souto, M. (2019). Fluvial-eolian deposits of the Tacuarembó Formation (Norte Basin - Uruguay): Depositional models and stratigraphic succession. *J. S. Am. Earth Sci.*, 90, 355–376.

Andò, S., Garzanti, E., Padoan, M., and Limonta, M. (2012). Corrosion of heavy minerals during weathering and diagenesis: A catalog for optical analysis. *Sed. Geol.*, 280, 165-178.

Bahlburg, H., Vervoort, J. D., Du Frane, S. A., Bock, B., Augustsson, C. and Reimann, C. (2009). Timing of crust formation and recycling in accretionary orogens: Insights learned from the western margin of South America. *Earth-Sci. Rev.*, 97(1-4), 215-241.

Baksi, A. K. (2018). Paraná flood basalt volcanism primarily limited to~ 1 Myr beginning at 135 Ma: New 40Ar/39Ar ages for rocks from Rio Grande do Sul, and critical evaluation of published radiometric data. *J. Volcanol. Geoth. Res.*, 355, 66-77.

Basei, M. A. S., Frimmel, H. E., Nutman, A. P., and Preciozzi, F. (2008). West Gondwana amalgamation based on detrital zircon ages from Neoproterozoic Ribeira and Dom Feliciano belts of South America and comparison with coeval sequences from SW Africa. *Geological Society*, London, Special Publications, 294(1), 239-256.

Bial, J., Buettner, S. H., Schenk, V. and Appel, P. (2015). The long-term high-temperature history of the central Namaqua Metamorphic Complex: Evidence for a Mesoproterozoic continental back-arc in southern Africa. *Precambrian Res.*, 268, 243-278.

Bigarella, J. J., and Salamuni, R. (1961). Early Mesozoic wind patterns as suggested by dune bedding in the Botucatu Sandstone of Brazil and Uruguay. *Geological Society of America Bulletin*, 72(7), 1089-1105.

Blott, S. J. and Pye, K. (2001). GRADISTAT: a grain size distribution and statistics package for the analysis of unconsolidated sediments. *Earth Surf. Proc. Land.*, 26(11), 1237-1248.

Canile, F. M., Babinski, M. and Rocha-Campos, A. C. (2016). Evolution of the Carboniferous-Early Cretaceous units of Paraná Basin from provenance studies based on U-Pb, Hf and O isotopes from detrital zircons. *Gondwana Res.*, 40, 142-169.

Cardenas, B. T., Kocurek, G., Mohrig, D., Swanson, T., Hughes, C. M., and Brothers, S. C. (2019). Preservation of Autogenic Processes and Allogenic Forcings in Set-Scale Aeolian Architecture II: The Scour-and-Fill Dominated Jurassic Page Sandstone, Arizona, USA. *J. Sed. Res*., 89(8), 741-760.

Casquet, C., Pankhurst, R. J., Rapela, C. W., Galindo, C., Fanning, C. M., Chiaradia, M., Baldo, E., González-Casado, J. M. and Dahlquist, J. A. (2008). The Mesoproterozoic Maz terrane in the Western Sierras Pampeanas, Argentina, equivalent to the Arequipa-Antofalla block of southern Peru: Implications for West Gondwana margin evolution. *Gondwana Research*, 13(2), 163-175.

Dias, K. D. N. and Scherer, C. M. (2008). Cross-bedding set thickness and stratigraphic architecture of aeolian systems: an example from the Upper Permian Pirambóia Formation (Paraná Basin), southern Brazil. *J. S. Am. Earth Sci.*, 25(3), 405-415.

Dickinson, W. R. and Gehrels, G. E. (2003). U–Pb ages of detrital zircons from Permian and Jurassic eolian sandstones of the Colorado Plateau, USA: paleogeographic implications. *Sed. Geol.*, 163(1-2), 29-66.

Dickinson, W. R., and Gehrels, G. E. (2010). Insights into North American paleogeography and paleotectonics from U–Pb ages of detrital zircons in Mesozoic strata of the Colorado Plateau, USA. *International Journal of Earth Sciences*, 99(6), 1247-1265.

Dickinson, W. R., and Gehrels, G. E. (2009). U-Pb ages of detrital zircons in Jurassic eolian and associated sandstones of the Colorado Plateau: Evidence for transcontinental dispersal and intraregional recycling of sediment. *Geological Society of America Bulletin*, 121(3-4), 408-433.

Dickinson, W. R. (1985). Interpreting provenance relations from detrital modes of sandstones. In.: *Provenance of arenites* (pp. 333-361). Springer, Dordrecht.

Ernesto, M., Raposo, M. I. B., Marques, L. S., Renne, P. R., Diogo, L. A., and De Min, A. (1999). Paleomagnetism, geochemistry and 40Ar/39Ar dating of the North-eastern Paraná Magmatic Province: tectonic implications. *Journal of Geodynamics*, 28(4-5), 321-340.

Farrant, A. R., Mounteney, I., Burton, A., Thomas, R. J., Roberts, N. M., Knox, R. W., and Bide, T. (2019). Gone with the wind: dune provenance and sediment recycling in the northern Rub'al-Khali, United Arab Emirates. *Journal of the Geological Society*, 176(2), 269-283.

França, A. B., Araújo, L. M., Maynard, J. B. and Potter, P. E. (2003). Secondary porosity formed by deep meteoric leaching: Botucatu eolianite, southern South America. *AAPG bulletin*, 87(7), 1073-1082.

Francischini, H., Dentzien–Dias, P. C., Fernandes, M. A. and Schultz, C. L. (2015). Dinosaur ichnofauna of the Upper Jurassic/Lower Cretaceous of the Paraná Basin (Brazil and Uruguay). *J. S. Am. Earth Sci.*, 63, 180-190.

Garzanti, E., Vermeesch, P., Vezzoli, G., Andò, S., Botti, E., Limonta, M., Dinis, P., Hahn, A., Baudet, D., De Grave, J. and Yaya, N. K. (2019). Congo River sand and the equatorial quartz factory. *Earth-Science Reviews*, 102918.

Garzanti, E., Vermeesch, P., Padoan, M., Resentini, A., Vezzoli, G., and Andò, S. (2014). Provenance of passive-margin sand (Southern Africa). *The Journal of Geology*, 122(1), 17-42.

Garzanti, E., Vermeesch, P., Andò, S., Vezzoli, G., Valagussa, M., Allen, K., Kadi, K.A. and Al-Juboury, A.I. (2013). Provenance and recycling of Arabian desert sand. *Earth-Sci. Rev.*, 120, 1-19.

Garzanti, E., Andò, S., Vezzoli, G., Lustrino, M., Boni, M. and Vermeesch, P. (2012). Petrology of the Namib Sand Sea: long-distance transport and compositional variability in the wind-displaced Orange Delta. *Earth-Sci. Rev.*, 112(3-4), 173-189.

Garzanti, E., Dinis, P., Vermeesch, P., Andò, S., Hahn, A., Huvi, J Limonta, M., Padoan, M., Resentini, A., Rittner, M. and Vezzoli, G. (2018). Dynamic uplift, recycling, and climate control on the petrology of passive-margin sand (Angola). *Sed. Geo.*, 375, 86-104.

Gehrels, G. (2014). Detrital zircon U-Pb geochronology applied to tectonics. *Annual Review of Earth and Planetary Sciences*, 42, 127-149.

Havholm, K. G., and Kocurek, G. (1994). Factors controlling aeolian sequence stratigraphy: clues from super bounding surface features in the Middle Jurassic Page Sandstone. *Sedimentology*, 41(5), 913-934.

Höfig, D. F., Marques, J. C., Basei, M. A. S., Giusti, R. O., Kohlrausch, C., and Frantz, J. C. (2018). Detrital zircon geochronology (U-Pb LA-ICP-MS) of syn-orogenic basins in SW Gondwana: New insights into the Cryogenian-Ediacaran of Porongos Complex, Dom Feliciano Belt, southern Brazil. *Precambrian Research*, 306, 189-208.

Hurst, A., Morton, A., Scott, A., Vigorito, M., and Frei, D. (2017). Heavy-Mineral Assemblages In.: Sandstone Intrusions: Panoche Giant Injection Complex, California. *J. Sed. Res.*, 87(4), 388-405.

Ingersoll, R. V., Bullard, T. F., Ford, R. L., Grimm, J. P., Pickle, J. D. and Sares, S. W. (1984) The effect of grain size on detrital modes: a test of the Gazzi-Dickinson point-counting method. *J. Sed. Res.*, 54(1), 103-116.

Janasi, V. A., Freitas, V. A. and Heaman, L. H. (2011). The onset of flood basalt volcanism, Northern Paraná Basin, Brazil: A precise U–Pb baddeleyite/zircon age for a Chapecó-type dacite. *Earth Planet. Sci. Lett.*, 302(1-2), 147-153.

Janikian, L., de Almeida, R. P., Fragoso-Cesar, A. R. S., de Souza Martins, V. T., Dantas, E. L., Tohver, E., and D'Agrella-Filho, M. S. (2012). Ages (U–Pb SHRIMP and LA ICPMS) and stratigraphic evolution of the Neoproterozoic volcano-sedimentary successions from the extensional Camaquã Basin, Southern Brazil. *Gondwana Res.*, 21(2-3), 466-482.
Jenisch, A. G., Lehn, I., Gallego, O. F., Monferran, M. D., Horodyski, R. S. and Faccini, U. F. (2017). Stratigraphic distribution, taphonomy and paleoenvironments of Spinicaudata in the Triassic and Jurassic of the Paraná Basin. *J. S. Am. Earth Sci.*, 80, 569-588.

Mange, M. A., and Maurer, H (2012). *Heavy minerals in colour*. Springer Science & Business Media.

Mcbride, E. F. (1985). Diagenetic processes that affect provenance determinations in sandstone. In.: *Provenance of arenites* (pp. 95-113). Springer, Dordrecht.

Milani, E. J., Melo, J. H. G., Souza, P. A., Fernandes, L. A. and França, A. B (2007). Bacia do Paraná. *Boletim de Geociências Petrobrás*, 15 (2), 265-287.

Milani, E. J., Faccini, U. F., Scherer, C. M. S., Araújo, L. M. and Cupertino, L. M. (1998). Sequences and stratigraphic hierarchy of the Paraná Basin (Ordovician to Cretaceous), Southern Brazil. Bol. IG USP, Série Científica, 29, 125-173.

Morton, A. C. and Hallsworth, C. (2007). Stability of detrital heavy minerals during burial diagenesis. *Developments in Sedimentology*, 58, 215-245.

Morton, A. C., and Hallsworth, C. (1994). Identifying provenance-specific features of detrital heavy mineral assemblages in sandstones. *Sed. Geol*, 90(3-4), 241-256.

Oriolo, S., Oyhantçabal, P., Basei, M.A., Wemmer, K. and Siegesmund, S. (2016). The Nico Pérez Terrane (Uruguay): from Archean crustal growth and connections

with the Congo Craton to late Neoproterozoic accretion to the Río de la Plata Craton. *Precambrian Res.*, 280, 147-160.

Oyhantçabal, P., Oriolo, S., Philipp, R. P., Wemmer, K. and Siegesmund, S. (2018a). The Nico Pérez Terrane of Uruguay and Southeastern Brazil. In *Geology of Southwest Gondwana* (pp. 161-188). Springer, Cham.

Oyhantçabal, P., Cingolani, C. A., Wemmer, K., and Siegesmund, S. (2018b). The Río de la Plata craton of Argentina and Uruguay. In.: *Geology of Southwest Gondwana* (pp. 89-105). Springer, Cham.

Oyhantçabal, P., Wagner-Eimer, M., Wemmer, K., Schulz, B., Frei, R. and Siegesmund, S. (2012). Paleo-and Neoproterozoic magmatic and tectonometamorphic evolution of the Isla Cristalina de Rivera (Nico Pérez Terrane, Uruguay). *International Journal of Earth Sciences*, 101(7), 1745-1762.

Perea, D., Soto, M., Veroslavsky, G., Martínez, S. and Ubilla, M. (2009). A Late Jurassic fossil assemblage in Gondwana: biostratigraphy and correlations of the Tacuarembó Formation, Parana Basin, Uruguay. *J. S. Am. Earth Sci.,* 28(2), 168-179.

Peri, V. G., Naipauer, M., Pimentel, M. and Barcelona, H. (2016). Eolian deposits of the shouthwestern margin of the Botucatú paleoerg: reconstruction of the Gondwana landscape in central northern Argentina. *Sed. Geol.*, 339, 234-257.

Philipp, R. P., Schultz, C. L., Kloss, H. P., Horn, B. L., Soares, M. B., and Basei, M. A. (2018). Middle Triassic SW Gondwana paleogeography and sedimentary dispersal revealed by integration of stratigraphy and U-Pb zircon analysis: the Santa Cruz Sequence, Paraná Basin, Brazil. *J. S. Am. Earth Sci.*, 88, 216-237.

Philipp, R. P., Pimentel, M. M. and Chemale Jr, F. (2016) Tectonic evolution of the Dom Feliciano Belt in Southern Brazil: geological relationships and U-Pb geochronology. *Brazilian Journal of Geology*, 46, 83-104.
Pinto, V. M., Hartmann, L. A., Santos, J. O. S., McNaughton, N. J., and Wildner, W. (2011). Zircon U–Pb geochronology from the Paraná bimodal volcanic province support a brief eruptive cycle at~ 135 Ma. *Chemical Geology*, 281(1-2), 93-102.

Pye, K., and Tsoar, H. (2008). Aeolian sand and sand dunes. Springer Science & Business Media.

Rahl, J. M., Reiners, P. W., Campbell, I. H., Nicolescu, S., and Allen, C. M. (2003). Combined single-grain (U-Th)/He and U/Pb dating of detrital zircons from the Navajo Sandstone, Utah. *Geology*, 31(9), 761-764.

Rapela, C. W., Pankhurst, R. J., Casquet, C., Baldo, E., Galindo, C., Fanning, C. M. and Dahlquist, J. M. (2010). The Western Sierras Pampeanas: Protracted Grenville-age history (1330-1030 Ma) of intra-oceanic arcs, subduction–accretion at continental-edge and AMCG intraplate magmatism. *J. S. Am. Earth Sci.*, 29(1), 105-127.

Resentini, A., Andó, S., and Garzanti, E. (2018). Quantifying roundness of detrital minerals by image analysis: Sediment transport, shape effects, and provenance implications. *J. Sed. Res.*, 88(2), 276-289.

Rittner, M., Vermeesch, P., Carter, A., Bird, A., Stevens, T., Garzanti, E., Andò, S., Vezzoli, G., Dutt, R., Xu, Z. and Lu, H. (2016). The provenance of Taklamakan desert sand. *Earth Planet. Sci. Lett.*, 437, 127-137.

Rossetti, L., Lima, E. F., Waichel, B. L., Hole, M. J., Simões, M. S., and Scherer, C. M.S. (2018). Lithostratigraphy and volcanology of the Serra Geral Group, Paraná-Etendeka Igneous Province in southern Brazil: Towards a formal stratigraphical framework. *J. Volcanol. Geoth. Res.*, 355, 98-114.

Saalmann, K., Gerdes, A., Lahaye, Y., Hartmann, L. A., Remus, M. V. D., and Läufer, A. (2011) Multiple accretion at the eastern margin of the Rio de la Plata craton: the prolonged Brasiliano orogeny in southernmost Brazil. *International Journal of Earth Sciences*, 100(2-3), 355-378.

Santos, J. O. S., Hartmann, L. A., Bossi, J., Campal, N., Schipilov, A., Piñeyro, D. and McNaughton, N. J. (2003). Duration of the Trans-Amazonian Cycle and its correlation within South America based on U-Pb SHRIMP geochronology of the La Plata Craton, Uruguay. *Int. Geol. Rev.*, 45(1), 27-48.

Sato, K., Basei, M. A. S., Ferreira, C. M., Sproesser, W. M., Vlach, S. R. F., Ivanuch, W. and Onoi, A. T. (2011). U-Th-Pb analyses by excimer laser ablation/ ICP-MS on MG Brazilian xenotime. *Goldschmidt Conference Abstracts*. Miner Mag 1801.

Scherer, C. M. and Goldberg, K. (2007). Palaeowind patterns during the latest Jurassic–earliest Cretaceous in Gondwana: Evidence from aeolian cross-strata of the Botucatu Formation, Brazil. *Palaeogeogr. Palaeoclimatol. Palaeoecol.*, 250(1-4), 89-100.

Scherer, C. M. and Lavina, E. L. (2006). Stratigraphic evolution of a fluvial–eolian succession: the example of the Upper Jurassic-Lower Cretaceous Guará and Botucatu formations, Paraná Basin, Southernmost Brazil. *Gondwana Research*, 9(4), 475-484.

Scherer, C. M. S. (2000). Eolian dunes of the Botucatu Formation (Cretaceous) in southernmost Brazil: morphology and origin. *Sed. Geol.*, 137(1-2), 63-84.

Scherer, C. M. S. (2002). Preservation of aeolian genetic units by lava flows in the Lower Cretaceous of the Paraná Basin, southern Brazil. *Sedimentology*, 49(1), 97-116.

Schneider, R. L., Muhlmann, H., Tommasi, E., Medeiros, R. A., Daemon, R. F. and Nogueira, A. A. (1973). **Revisão estratigráfica de Bacia do Paraná** An. XXVIII Congr. Bras. Geol., Soc. Bras. Geol., 1, pp. 41-65.

Soto, M. and Perea, D. (2008). A ceratosaurid (Dinosauria, theropoda) from the late Jurassic-Early Cretaceous of Uruguay. *Journal of Vertebrate Paleontolology*, 28(2), 439-444.

Thiede, D. S., and Vasconcelos, P. M. (2010). Paraná flood basalts: rapid extrusion hypothesis confirmed by new 40Ar/39Ar results. *Geology*, 38(8), 747-750.

Vermeesch, P., Resentini, A. and Garzanti, E. (2016) An R package for statistical provenance analysis. *Sed. Geol.*, 336, 14-25.

Wildner, W., Ramgrab, G. E., Lopes, R. C. and Iglesias, C. M. F. (2006). Mapa geológico do Estado do Rio Grande do Sul, Escala 1:750.000. CPRM - Companhia de Pesquisa de Recursos Minerais, Porto Alegre.

Zalán, P. V., Wolff, S. J. C. J., Conceição, J. D. J., Marques, A., Astolfi, M. A. M., Vieira, I. S., Appi, V. T. and Zanotto, O. A. (1990). Bacia do Paraná. *Origem e evolução das bacias sedimentares*, pp.135-168.

Zerfass, H., Lavina, E. L., Schultz, C. L., Garcia, A. J. V., Faccini, U. F. and Chemale Jr, F. (2003). Sequence stratigraphy of continental Triassic strata of Southernmost Brazil: a contribution to Southwestern Gondwana palaeogeography and palaeoclimate. *Sed. Geol.*, 161(1-2), 85-105.